Since January 2020 Elsevier has created a COVID-19 resource centre with free information in English and Mandarin on the novel coronavirus COVID-19. The COVID-19 resource centre is hosted on Elsevier Connect, the company's public news and information website.

Journal Pre-proof

A third dose of the unmodified COVID-19 mRNA vaccine CVnCoV enhances quality and quantity of immune responses

Klara Lenart, Fredrika Hellgren, Sebastian Ols, Xianglei Yan, Alberto Cagigi, Rodrigo Arcoverde Cerveira, Inga Winge, Jakub Hanczak, Stefan O. Mueller, Edith Jasny, Kim Schwendt, Susanne Rauch, Benjamin Petsch, Karin Loré

PII: S2329-0501(22)00143-7

DOI: https://doi.org/10.1016/j.omtm.2022.10.001

Reference: OMTM 943

To appear in: *Molecular Therapy: Methods & Clinical Development*

Received Date: 4 August 2022

Accepted Date: 4 October 2022

Please cite this article as: Lenart K, Hellgren F, Ols S, Yan X, Cagigi A, Cerveira RA, Winge I, Hanczak J, Mueller SO, Jasny E, Schwendt K, Rauch S, Petsch B, Loré K, A third dose of the unmodified COVID-19 mRNA vaccine CVnCoV enhances quality and quantity of immune responses, *Molecular Therapy: Methods & Clinical Development* (2022), doi: https://doi.org/10.1016/j.omtm.2022.10.001.

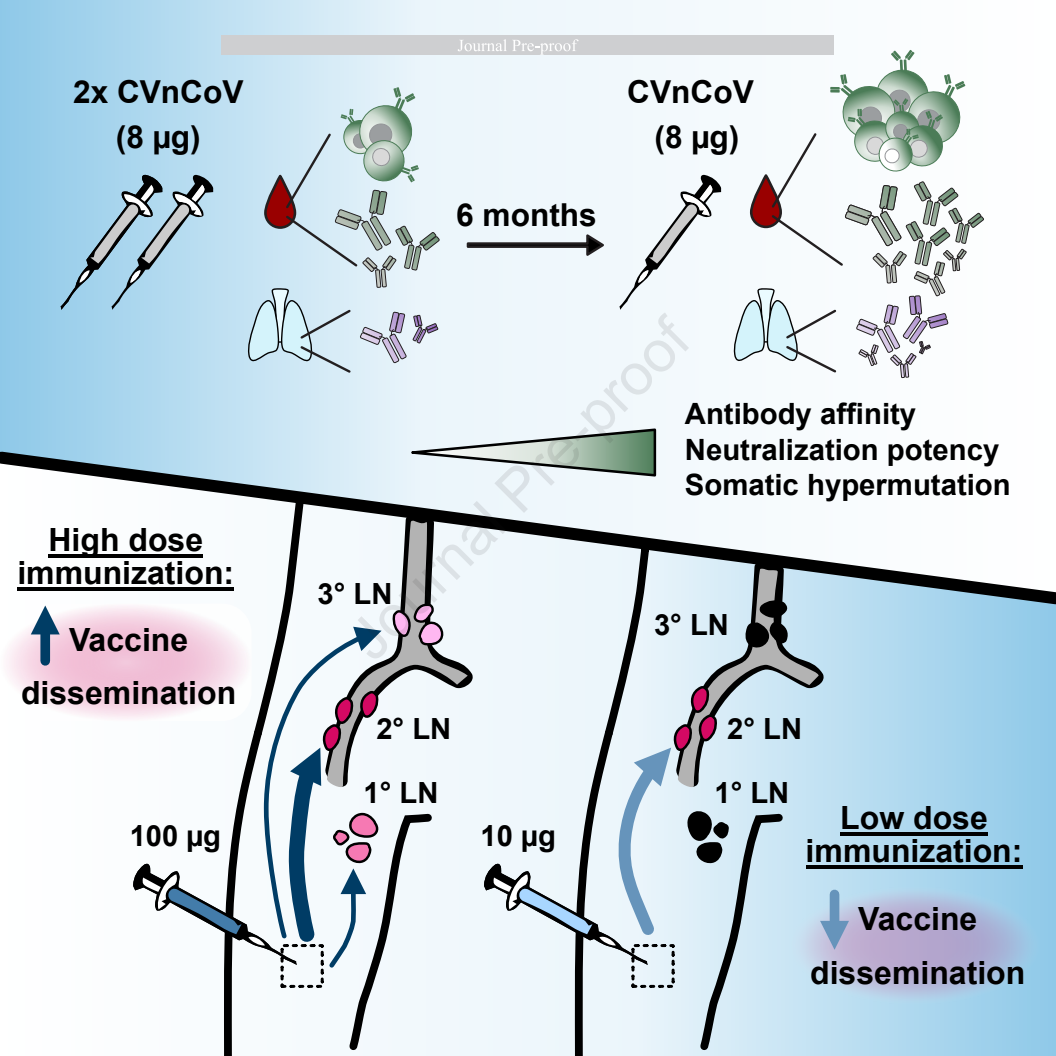

A third dose of the unmodified COVID-19 mRNA vaccine CVnCoV enhances quality and quantity of immune responses

Authors: Klara Lenart[1,2], Fredrika Hellgren[1,2], Sebastian Ols[1,2], Xianglei Yan[1,2], Alberto Cagigi[1,2], Rodrigo Arcoverde Cerveira[1,2], Inga Winge[1,2], Jakub Hanczak[1,2], Stefan O. Mueller[3], Edith Jasny[3], Kim Schwendt[3], Susanne Rauch[3], Benjamin Petsch[3], Karin Loré[1,2]

Affiliations

1. Department of Medicine Solna, Division of Immunology and Allergy, Karolinska Institutet and Karolinska University Hospital, Stockholm, Sweden.
2. Center for Molecular Medicine, Karolinska Institutet, Stockholm, Sweden.
3. CureVac AG, Tübingen, Germany.

Correspondence should be addressed to:

Karin Loré,
Division of Immunology and Allergy, Department of Medicine Solna,
Karolinska Institutet,
Visionsgatan 4, BioClinicum J7:30, Karolinska University Hospital,
171 64 Stockholm, Sweden.
E-mail address: karin.lore@ki.se

Short title: A third dose of CVnCoV enhances immune responses (48 characters)

Abstract – limit = 200 words, actual = 199

Main body text = 4,381

Methods text = 2,497

ABSTRACT

A third vaccine dose is often required to achieve potent, long-lasting immune responses. We investigated the impact of three 8 μg doses of CVnCoV, CureVac's SARS-CoV-2 vaccine candidate containing sequence-optimized unmodified mRNA encoding spike (S) glycoprotein, administered at 0, 4 and 28 weeks on immune responses in rhesus macaques. Following the third dose S-specific binding and neutralizing antibodies increased 50-fold compared with post-dose 2 levels, with increased responses also evident in the lower airways and against the SARS-CoV-2 B.1.1.7 (Alpha), B.1.351 (Beta), P.1 (Gamma) and B.1.617.2 (Delta) variants. Enhanced binding affinity of serum antibodies after the third dose correlated with higher somatic hypermutation in S-specific B cells, corresponding with improved binding properties of monoclonal antibodies expressed from isolated B cells. Administration of low dose mRNA led to fewer cells expressing antigen *in vivo* at the injection site and in the draining lymph nodes compared with a tenfold higher dose, possibly reducing the engagement of precursor cells with the antigen and resulting in the suboptimal response observed following two-dose vaccination schedules in phase IIb/III clinical trials of CVnCoV. However, when immune memory is established, a third dose efficiently boosts the immunological responses as well as improves antibody affinity and breadth.

Word count abstract: 199

INTRODUCTION

The COVID-19 pandemic resulted in an accelerated development of vaccines against severe acute respiratory syndrome coronavirus-2 (SARS-CoV-2), with 38 approved vaccines in 197 countries and 212 candidates in testing as of June 2022.[1] Most notable of these were two nucleoside modified mRNA vaccines (BNT162b2; BioNTech/Pfizer and mRNA-1273; Moderna) which were rapidly authorized, manufactured and distributed while several other sequence-optimized chemically unmodified mRNA vaccines are still in clinical development.[1] CureVac's vaccine candidate, CVnCoV, was the first unmodified mRNA SARS-CoV-2 vaccine to reach phase III clinical testing.[2] In the reported clinical trials of CVnCoV much lower doses of unmodified mRNA (2–12 μg) were tested than those used in modified mRNA vaccines, e.g. 30 μg in the BioNTech/Pfizer[3] and 100 μg in the Moderna vaccines.[4] This was because unmodified mRNA vaccines are considered to induce stronger innate immune activation which, at high doses, may lead to reactogenicity. Indeed, a trend for a dose-dependent increase in local and systemic solicited events was observed in the phase 1 dose-escalation study of CVnCoV.[5]

In the phase IIb/III HERALD trial the CVnCoV vaccine candidate containing 12 μg mRNA encapsulated in lipid nanoparticles (LNP) showed an overall vaccine efficacy (VE) of 48.2% against COVID-19 of any severity and 70.7% against moderate-to-severe COVID-19, measured in an environment with 15 different circulating SARS-CoV-2 variants.[2] CureVac decided to discontinue development of CVnCoV and focus on new generation candidates.[6]

To inform the development of better strategies for immunization with more efficacious vaccine candidates, we performed a detailed immunological investigation to understand the magnitude and quality of the immune responses to CVnCoV including an assessment of the impact of a third 8 μg dose of CVnCoV on the immune response in non-human primates

(NHPs). The NHP model allowed us to take multiple samples over time, and to collect not only blood samples but also respiratory samples for assessment of mucosal responses and bone marrow for long-lived plasma cell responses. In a two dose vaccination schedule 8 μg CVnCoV has been shown to induce seroconversion, but with relatively low antibody titers both in humans[5] and NHPs.[6–8] However, in NHP challenge studies partial protection against SARS-CoV-2 was achieved indicating protective immunity had been established. The NHP model therefore offers an opportunity to perform high resolution analyses in a physiologically relevant setting.

RESULTS

CVnCoV administration rapidly induced type I interferon-polarized and transient innate immune activation

We measured multiple aspects of the immune response induced by CVnCoV including immediate responses after administration as well as long-term adaptive responses. Three rhesus macaques were immunized with 8 μg CVnCoV encapsulated in LNPs at weeks 0 and 4, followed by a booster dose at week 28. Peripheral blood and bronchoalveolar lavage (BAL) samples were collected over the 37-week study period and bone marrow aspirates were collected following euthanasia at study end (Fig. 1A).

Within 24 hours of immunization, markers of innate immune activation and toxicity showed either no or only minor transient fluctuations that remained within the normal range of the clinical chemistry and complete blood counts (CBCs) (Fig. S1A-B). Animals did not show any behavioral changes, increase in body temperature or long-term weight differences. By combining CBC and phenotyping by flow cytometry (Fig. 1B) we were able to detect a transient decrease in circulating lymphocytes including T cells, B cells, NK cells and NKT cells 24 hours after immunization (Fig. S1C), coinciding with an elevated proportion of

circulating monocytes (Fig. 1C). This increase was mainly represented by CD14+ CD16+ intermediate monocytes (Fig. 1D) which is consistent with previous reports on intermediate monocyte expansion following administration of TLR7/8-based adjuvants or mRNA vaccines.[9–11] Most of the 30 plasma analytes measured showed no or very low increases 24 hours after CVnCoV administration (Fig. 1E). However, in line with the transient increase in intermediate monocytes, elevated levels of the monocyte attractant protein-1 (MCP-1; CCL2) were detected at 24 hours (Fig. 1E-F). In addition, interleukin 1 receptor antagonist (IL-1RA) was induced as well as cytokines associated with a type I interferon (IFN) response such as IFN-α and CXCL11 (Fig. 1E-F). All cytokines had returned to baseline levels by Day 14 (Fig. 1E-F). No detectable levels of classical inflammatory cytokines such as TNF-α and IL-6 were induced. Principal component analysis (PCA) of the 30 plasma analytes confirmed differences between baseline and 24 hour samples mainly due to type I IFN-associated cytokines, MCP-1 and IL-1RA (Fig. 1G). Collectively, this demonstrated that systemic innate immune activation was induced by CVnCoV with limited and transient adverse events.

A third dose increased the levels of neutralizing and cross-reactive antibodies

Using the 8 μg dose of CVnCoV, we found low but detectable antibody titers against SARS-CoV-2 S protein and the receptor-binding domain (RBD) of the S protein at week 6, two weeks after the second dose (Fig. 2A). In clinical studies, suboptimal efficacy elicited by immunization with two doses of CVnCoV, ultimately led to a halt in clinical development. We therefore investigated the potential of a third dose to increase the responses. The animals received a third dose 24 weeks (six months) after the second dose, a relevant time frame for a human booster dose. Titers increased significantly following the third (booster) dose, which is in line with the kinetics of antibody responses in the clinical trial testing the booster potential of the third CVnCoV immunization.[12] Two weeks after the third dose, binding titers for S protein and RBD were respectively 12.8- and 6.4-fold higher than peak titers two weeks

after the second dose (Fig. 2A). The boosting effect was even stronger for neutralizing (Fig. 2B) and pseudovirus neutralizing titers (Fig. 2C). These titers increased by 33.6- and 23.7-fold, respectively, and matched the neutralization capacity of the WHO international standard (NIBSC 20/136), which was not the case after the first two immunizations (Fig. 2B). This large change in response from the second to the third dose for neutralization of ancestral (WA-1) SARS-CoV-2 virus has not been reported for the licensed mRNA vaccines mRNA-1273 and BNT162b2, although titers were higher after the first two doses.[13–16] While showing that low dose CVnCoV can elicit high responses with three immunizations, mean responses after three doses were still lower than those reported with the 30–100 μg doses of licensed mRNA vaccines in NHP models[17,18] or clinical studies,[19,20] although differences between the assays used have to be considered.

The significant increase in titers after the CVnCoV third dose was also reflected in higher neutralization potency, defined as the ratio between the neutralizing and the binding titers (Fig. 2D).[13] This suggests not only a substantial improvement in titers but also in antibody quality; however as the group size was small and one animal persistently showed lower responses this difference was not significantly different.

In a recent study, S protein was detected in the serum of BNT162b2 vaccinees after the first, but not the second dose due to masking of S epitopes by the serum antibodies.[16] In our NHP sera, S protein was detectable 24 hours after the first dose in all three animals, while only the animal with the lowest S-specific titers had systemically detectable S protein 24 hours after the third dose (Fig. 2E).

In addition to the large increase in antibody response to the ancestral S protein following the third dose, antibody titers against S proteins from the SARS-CoV-2 B.1.1.7 (Alpha), B.1.351 (Beta), P.1 (Gamma) and B.1.617.2 (Delta) variants were also increased (Fig. 2F). The

147 increase following the third dose was also demonstrated by higher ratios between variant and
148 ancestral binding titers (Fig. 2G).

149 While serum antibodies are often used to assess vaccine responses and predict correlates of
150 protection[21–23] it is likely that mucosal immunity to SARS-CoV-2 is necessary to prevent
151 infection and mild disease. Anti-S and RBD-binding IgG and neutralizing titers in
152 bronchoalveolar lavage fluid (BAL) were barely detectable two weeks after the second dose,
153 but as with serum antibodies, they were strongly boosted after the third dose (Fig. 2H-I).
154 There was a strong correlation between antibody levels in BAL and in plasma ($r = 0.8441$, $p < 0.001$) (Fig. 2J), suggesting that mucosal antibodies may predominantly transudate from
156 serum as previously proposed.[21]

157 Antibody-secreting S and RBD-specific plasmablasts were undetectable after the two priming
158 immunizations but were detectable by enzyme-linked immunospot (ELISpot) four days after
159 the third dose (Fig. 2K). S protein and RBD-specific plasma cells in the bone marrow were
160 found at week 37 (study end; Fig. 2L) suggesting that the animals had generated vaccine-
161 specific B cell populations critical to establish longevity of the antibody response. S-specific
162 memory T cells, assessed by antigen recall assay using stimulation with overlapping S
163 peptides and intracellular cytokine production (Fig. S2A-B), showed low but detectable $CD4^+$
164 T cell responses after the second dose in blood and in BAL (Fig. 2M). These responses
165 waned but were boosted by the third dose, especially in the BAL. The T cell response was
166 Th1 polarized as shown by IFN-γ and IL-2 production but a proportion of IL-21-producing
167 circulating T follicular cells was also detected, especially two weeks after the third dose (Fig.
168 2N). Low frequencies of IFN-γ producing $CD8^+$ T cell responses were detectable in both
169 blood and BAL (Fig. 2O).

170 In conclusion, a third dose 24 weeks after the two-dose primary series amplified the initial
171 vaccine responses. A strong increase in antibody titers resulting in improved neutralization of

and binding to the ancestral strain as well as variant strains, and higher mucosal responses, was accompanied by the induction of S-specific IL-21 secreting circulating T follicular helper and Th1 memory cells.

The third immunization drives affinity maturation of vaccine-specific B cells

S-specific circulating memory B cells measured by binding to fluorescently labeled S using flow cytometry (Fig. 3A, Fig. S3A) showed a clear increase in frequency after the second immunization. Despite the expected waning, S-specific memory B cells remained at detectable levels for 24 weeks (Fig. 3B). The third immunization resulted in a clear expansion with readily detectable levels until study end. Of the S-specific memory B cells, only 11.1% (range 0–30.3%) were specific to RBD throughout the study as previously reported (Fig. 3C).[24–26] Conversely, on average 64.9% (range 33–79%) of the antibodies in plasma were RBD-reactive (Fig. 3D, Fig. S3B-C), similar to the proportions observed in convalescent individuals.[27] This discrepancy in the memory B cell pool and circulating antibodies may reflect differences between the antibody producing plasma cells in the bone marrow compartment and memory B cells. Over time and with the third immunization, we observed that although the proportion of RBD-specific antibodies decreased slightly they still represented the majority of the response (Fig. 3D).

To determine whether there were qualitative differences in affinity maturation and epitope-specificities in vaccine-elicited B cell responses, we single-cell sorted S-specific memory B cells obtained two weeks after the second and third immunizations and sequenced the variable regions of the heavy (VH) and light (VL) chains of their B cell receptors. Productive, high-quality sequences were obtained from a total of 444 single memory B cells (155 and 289 after the second and third immunizations, respectively). The level of somatic hypermutation (SHM) in the VH region was calculated after alignment with the largest germline IGHV allele database available based on multiple rhesus macaques.[28] Significantly higher SHM was

found in the memory B cells after the third immunization compared with the second (Fig. 3E). Along with the increase in SHM after the third dose, we found that antibody binding avidity increased significantly at week 30 in agreement with a recent report.[29] High avidity remained stable until study end, a further indication of a qualitative improvement of the humoral response (Fig. 3F).

The memory B cell response was highly polyclonal with the majority of the sequences belonging to independent lineages (defined as the same IGHV and IGHJ allele, same HCDR3 length, 80% amino acid identity in the HCDR3 and one identical HCDR3 junction) (Fig. S3D). However, several lineages were detected at both weeks 6 and 30 (labelled in the same color in Fig. S3D) indicating that they were maintained and expanded by the third dose. To further investigate maturation of the B cell response following the third dose, we selected 10 sequence pairs from the lineages that were detected at both weeks 6 and 30 and expressed them as monoclonal antibodies (mAbs). These selected lineages did not expand within the sampled B cell repertoire with the third dose (Fig. S3E-F) but they showed significant affinity maturation (Fig. 3G). This confirms the increased SHM as found in the memory B cell pool at large.

Although 16 out of the 20 mAbs we expressed bound S protein, only two (from the same lineage) bound the S1 domain and none of them bound RBD alone (Fig. 3H). Therefore, we predict most expressed mAbs bind the S2 subunit (Fig. 3K), which is rarely a target of neutralizing antibodies. This corroborates our data on expansion of non-RBD-specific memory B cells with the boost immunization. Furthermore, high proportions of S2-specific B cells were previously reported following SARS-CoV-2 infection[30] and vaccination.[31] Expressed mAbs isolated from B cells at week 30 showed significantly better binding to S protein than the related sequences isolated at week 6 (Fig. 3I). Moreover, the mAbs from week 30 exhibited a trend towards higher avidity indices, which were comparable to well-

characterized reference mAbs specific for NTD or RBD of ancestral S protein (Fig. 3J). Collectively, this shows a clear maturation of the B cell response with the third vaccine dose demonstrated on antibody and memory B cell level.

A higher mRNA vaccine dose increases dissemination to more lymph nodes

We and others have shown in NHPs that mRNA vaccine administration leads to local inflammation in the muscle at the site of injection consisting of infiltration of immune cells, including antigen presenting cells, uptake and translation of the mRNA.[32,33] The efficiency of this process is probably impacted by the dose of vaccine, so the low dose used in our study may have limitations in the number of cells infiltrating the injection site and becoming available as target cells for the vaccine as well as for disseminating vaccine antigen. This would have consequences for the initiation of an adequate vaccine-specific response. We used an mRNA construct based on sequence-optimized unmodified mRNA encoding the fluorescent protein mCitrine that enabled identification of mRNA translation in cells. The mRNA construct was formulated in DiD-labeled LNPs allowing us to track LNP uptake independently from mRNA translation. By exposing isolated monocytes to 5 μg/mL mRNA/LNP *in vitro*, we found detectable LNP uptake already after a 6 hour incubation (Fig. 4A-B). mCitrine expression was slightly delayed compared with LNP uptake but was detectable at 24 hours, and high levels of mCitrine+ cells remained detectable for at least 3 days. Using a tenfold higher dose of the construct did not result in higher LNP uptake, but we did observe a dose-dependent pattern of mCitrine expression *in vitro*.

We then investigated whether differences in doses significantly affected biodistribution and antigen expression *in vivo*, mimicking low dose CVnCoV administration. Rhesus macaques received intramuscular injections of low (10 μg) or high (100 μg) doses of the labeled LNP/mCitrine mRNA construct (Fig. 4C) with intramuscular saline injections as controls. The animals were injected at four different sites simultaneously (left and right deltoid and

247 quadricep muscles), allowing for the direct comparison of saline versus mRNA vaccine
248 administration in the same animal. This enabled collection of multiple data points from each
249 animal while limiting the number of animals used. Injection site muscle biopsies were taken
250 after 24 hours, as we have previously observed that there is high level of antigen uptake and
251 local innate immune activity at this timepoint.[32,34,35] To identify which lymph nodes (LNs)
252 were primarily targeted by mRNA vaccination, several LN clusters were collected and
253 classified as the primary (1°; axillary or inguinal), secondary (2°; apical or iliac) or
254 tertiary/third (3°; supraclavicular or paraaortic) draining LNs based on their proximity to the
255 injection site (Fig. 4C). We analyzed early immune processes critical for initiation of
256 adaptive responses such as cell infiltration, vaccine uptake and translation and further
257 dissemination to lymph nodes.

258 When compared with the control tissues there was noticeable recruitment of CD45+ immune
259 cells to the LNP/mRNA injected sites as well as into the draining lymph nodes specifically in
260 a dose-dependent manner (Fig. 4D). Multiple cell subsets were defined within the CD45+
261 immune cells (Fig. S4A). CD66abce+ neutrophils, classical CD14+ CD16- monocytes and
262 myeloid dendritic cells (mDCs) were the most frequent cell types infiltrating the muscle
263 injection site (Fig. 4E), with some infiltration of the muscle by plasmacytoid DCs, T cells, B
264 cells and NK cells. Of these, monocytes exhibited the most pronounced dose-dependent
265 accumulation in the draining lymph nodes after mRNA vaccine administration (Fig. 4E-F).

266 mDCs and monocytes play an essential role in antigen presentation and maintaining adaptive
267 responses. Using mRNA encoding for mCitrine we determined the target immune cells for
268 the LNP/mRNA vaccine (Fig. 4G). No LNP+ or mCitrine+ cells were detected at the saline-
269 injected control sites demonstrating that the uptake and translation is restricted to the
270 vaccination sites and their draining LNs (Fig. 4G-H). Although we observed that non-
271 immune CD45- cells in muscle tissue were able to take up LNP and translate mRNA into

protein (Fig. S4B), the production of mCitrine was much less efficient compared with CD45+ immune cells. Monocytes were found to be the most abundant LNP+ mCitrine+ immune cells (Fig. 4H), with both classical CD14+ CD16- and intermediate CD14+ CD16+ subsets infiltrating the site of injection, although classical monocytes were the predominant vaccine+ subset in the draining lymph nodes (Fig. 4K). In addition, mDCs also showed clear LNP uptake and mCitrine translation (Fig. 4G-H). Importantly, we observed that a tenfold higher dose of vaccine led to a broader mRNA dissemination evidenced by LNP+ mCitrine+ monocytes in more draining LN clusters (Fig. 4I).

In contrast to the clear expression of mCitrine in monocytes and mDCs, neutrophils were efficient at internalizing LNP but not at translating the mRNA (Fig. 4G-H) in accordance with our earlier data.[33] Other immune cells, such as T cells, B cells and plasmacytoid DCs, showed low signals for both LNP and mCitrine in comparison with monocytes and mDCs (Fig. S4C). There was a correlation between the number of infiltrating monocytes in the muscle and the number of mCitrine+ monocytes both in primary and secondary draining lymph nodes (Fig. 4J). Altogether this demonstrates that a sequence-optimized unmodified mRNA vaccine has a similar pattern of biodistribution and cell-specific targeting as that reported for modified mRNA vaccines, but a low dose of mRNA results in restricted dissemination to the secondary lymphoid organs compared with a higher dose.

DISCUSSION

The 48.7% efficacy against COVID-19 of any severity observed in the phase IIb/III clinical trial of CVnCoV was followed by the decision to reorient the development of this vaccine candidate. However, the results from this NHP study showed that a third CVnCoV dose significantly enhanced both the magnitude and the quality of the immune response compared with two doses. Although the average neutralizing antibody responses after three 8 μg doses

297 of CVnCoV were numerically lower than those reported with the 30–100 μg doses of the
298 licensed mRNA vaccines in NHPs[17,18] or humans,[19,20] the marked fold increase in
299 neutralizing activity against ancestral SARS-CoV-2 after the third dose, compared with after
300 the second dose, was substantially higher than that reported for three doses of the licensed
301 mRNA vaccines mRNA-1273 and BNT162b2.[13–15] Establishment of vaccine-specific plasma
302 cells in the bone marrow after the third dose, combined with neutralizing serum antibody
303 titers in the range of WHO international standard 2.5 months after the last dose, suggest that
304 three CVnCoV doses elicit durable immune responses beyond the investigated study period.
305 Similarly to immunization with BNT162b2,[16] we detected S protein in sera of CVnCoV
306 vaccinated NHPs 24 hours after administration but at a concentration 10-fold lower than that
307 observed in BNT162b2 vaccinees. This may reflect the overall antigen load and impact the
308 development of the vaccine responses, although the physiological differences in size and
309 weight between humans and NHPs need to be considered. Our study results suggest that a
310 third CVnCoV dose provides an efficient boosting of the immune responses once SARS-
311 CoV-2-specific memory has been established and importantly, it provides mechanistic
312 information about how this boosting effect is brought about. In recent clinical studies,
313 CVnCoV performed well as a booster vaccine in previously vaccinated individuals,[12,36]
314 eliciting superior antibody titers compared to Valneva's Alum/CpG-adjuvanted inactivated
315 vaccine candidate VLA2001, albeit inferior responses to licensed mRNA vaccines.[36]
316 Importantly, we found clear evidence of qualitative enhancement of the responses in plasma
317 antibodies and the B cell repertoire manifested by higher binding avidity and SHM,
318 respectively. We have also shown that the third immunization enhanced cross-reactivity of
319 plasma antibodies to several variant Spike proteins, which is relevant in the light of
320 continuing emergence of new variants with divergent mutations in the S-protein.[37]

The suboptimal responses to CVnCoV in clinical trials spurred the development of the next generation vaccine candidate, CV2CoV. This updated version of CVnCoV contains unmodified nucleosides but with optimized non-coding regions and has been reported to induce higher titers of binding and neutralizing antibodies, memory B cell responses and T cell responses as well as more robust protection compared with CVnCoV when two doses were administered four weeks apart in NHPs.[8] The S-specific antibody and B and T cell responses after the third dose of CVnCoV found in our study were in a range similar to that found for CV2CoV after two doses. Although our study did not include virus challenge, the serum neutralizing titers after the third dose were consistent with titers reported in other studies that provided significant protection in challenge experiments.[8,38] Based on this published data, protection from infection would persumaby be higher after three doses of CVnCoV compared with two, and in the range observed with CV2CoV. However, CV2CoV also induced higher levels of type I IFN responses and MIP-1α 24 hours after immunization compared with CVnCoV. This needs to be further evaluated since undesired side-effects due to innate immune activation have been a concern with unmodified mRNA vaccines.

The first unmodified mRNA vaccine tested in humans was against rabies virus in which about 78 % of study participants reported transient mild-to-moderate systemic side effects after administration of protamine-complexed mRNA.[39] More recently, in a phase 1 clinical trial considerable side-effects were reported with 5 μg unmodified rabies mRNA in LNPs while 1 or 2 μg doses were well tolerated and elicited immune responses comparable with those of a licensed rabies vaccine.[40] This data on dosing contributed to the design of the doses selected for CVnCoV, which also displayed dose-dependent increases in reactogenicity up to the maximum dose of 12 μg tested.[5]

The innate immune activation characterized by type I IFN responses following mRNA vaccination likely plays an important role in the immunogenicity of the mRNA platform and

its Th1 polarized profile of adaptive responses.[34,41,42] Type I IFN responses have been shown to directly support B cell differentiation and survival resulting in enhanced antibody responses.[43,44] Increased antibody half-life and durability of humoral responses have been shown with type I IFN-inducing adjuvants such as TLR3, 7/8 and 9-ligands (poly IC:LC, R848, CpG).[45–48] In the current study, we observed that CVnCoV induced a strong, transient type I IFN response (IFNα, CXCL11) as well as monocyte activation evidenced by MCP-1 induction and intermediate monocyte differentiation within 24 hrs of administration. A similar activation profile after administration of nucleoside-modified mRNA vaccines has been reported previously.[11,32,49] Intermediate monocytes have been shown to be important for antigen presentation to $CD4^+$ T cells[50] and to support the differentiation of naïve B cells into antibody-secreting plasmablasts.[51,52]

Little is known about the mechanisms of action by which LNP/mRNA-based vaccines generate strong vaccine responses. Using an *in vitro* experimental approach, we showed that lower doses of mRNA led to detectable protein production in fewer monocytes compared with higher doses. Antigen availability is an important determinant for the outcome of the germinal center reaction[53] and a low protein translation rate could result in less protein antigen being available to support the germinal center reaction, thereby limiting the B cell response. Another major observation in our study is that sequence-optimized unmodified and modified mRNA/LNP vaccine formulations appear to have a similar biodistribution pattern and cell-specific targeting. Our *in vivo* biodistribution data showed that a lower dose resulted in a limited spread of the vaccine-positive immune cells and fewer targeted LNs, demonstrating restricted vaccine dissemination. This restricted dissemination would have a greater impact in a primary immunization setting where the induction of vaccine-specific immune responses relies on encounters between the vaccine and sparse antigen-specific naïve

lymphocytes, than in a booster setting, when memory B and T cell pools would already have been established.

Although this study has obvious limitations due to having only three animals per group, we followed the animals with multiple samplings over eight months and we were able to analyze numerous aspects of the immune responses. Therefore, we were able to study the evolution of the vaccine responses over a significant time period with control measurements from the same individual. We mapped antibody responses in detail and monitored the emergence of S-specific memory B cells over time. After two doses, most serum antibodies were RBD-specific. The third immunization had a particular effect of expanding the immune response against non-RBD epitopes, proportions of which remained stable until study end. This is important as SARS-CoV-2 vaccination has been shown to induce responses that are dominated by non-neutralizing antibodies[54,55] and while animal studies have shown that non-neutralizing antibodies can contribute to protection,[56,57] clinical studies have shown that serum neutralizing antibody titer strongly correlates with vaccine-induced efficacy against symptomatic COVID-19.[23,58] In this study NHPs developed high titers of neutralizing antibody titers after the third dose. However, none of the mAbs we expressed from the S-specific circulating memory B cell pool were RBD-reactive. This probably reflects the high representation of non-RBD-specific clones in the B cell repertoire as reported elsewhere,[55,59] and warrants further investigation of immunization strategies to expand the RBD-specific B cell repertoire.

Our study in NHPs adds important mechanistic information on CVnCoV including the use of a three-dose immunization regimen which has been recently reported in a clinical trial.[12,60] Our data will complement those observed in human volunteers to elucidate the mechanism of action of CVnCoV and inform development of an improved version for future use.

METHODS

Vaccines

The CVnCoV vaccine candidate is based on the RNActive® platform. It has a 5′ cap structure, 5'UTR, a GC-enriched open reading frame, 3′ UTR, polyA tail and has no chemically modified nucleosides. The mRNA was encapsulated using the lipid nanoparticle (LNP) technology of Acuitas Therapeutics (Vancouver, Canada). The LNPs used in this study are particles of ionizable amino lipid, phospholipid, cholesterol and a PEGylated lipid. The mRNA encoded protein is based on the S-protein of SARS-CoV-2 NCBI Reference Sequence NC_045512.2, GenBank accession number YP_009724390.1 and encodes for full length S-protein featuring K986P and V987P mutations. mRNA encoded protein for mCitrine is based on the description by Griesbeck *et al.*[61]

Immunogenicity study design and sample collection

Three female Chinese rhesus macaques (*Macaca mulatta*, 12-13 years old) were used in this study. They were housed in the Astrid Fagraeus Laboratory at Karolinska Institutet, Stockholm. All animal experiments were conducted following the guidelines and regulations of the Association for Assessment and Accreditation of Laboratory Animal Care and the Swedish Animal Welfare Agency. The study was approved by the Regional animal ethics committee of Northern Stockholm. The animals received intramuscular (i.m.) injections of 8 µg doses of CVnCoV in their left quadriceps at weeks 0, 4 and 28. Heparinized peripheral blood, serum and bronchoalveolar lavage (BAL) samples were collected over the 37-week study period and bone marrow aspirates were collected following euthanasia at the end of this period. Body weight and temperature were monitored at each sampling timepoint. CBCs and clinical chemistry analyses were performed at baseline, then 24 hours and 14 days after the first and third doses by Adlego Biomedical (Solna, Sweden). Clinical chemistry was performed on an ABAXIS Vetscan VS2 3.1.35 Chemistry analyzer using Mammalian Liver Profile rotors (Triolab, Solna, Sweden).

Sample processing

Peripheral blood mononuclear cells (PBMCs) were isolated by standard gradient density centrifugation from heparinized blood using Ficoll-Pacque (GE Healthcare). PBMCs were used either immediately for downstream applications or cryopreserved in 10% dimethyl sulfoxide (DMSO)/fetal calf serum (FCS) until use.

BAL cells were separated from the supernatant by centrifugation. Cells were passed through a 70 μm cell strainer and used fresh in a T cell stimulation assay. Supernatants were stored separately and concentrated tenfold using Amicon-Ultra centrifugal filter units with 30 kDa cut-off (Millipore) before downstream analysis.

Innate response flow cytometry

Immune cell subsets in peripheral blood were monitored by flow cytometry on days 0, 1 and 14 after the first and third doses. Freshly isolated PBMCs were stained with Live/Dead™ Fixable Blue Dye (Life technologies) and FcR blocking reagent (Miltenyi Biotec), followed by a panel of antibodies for innate immunophenotyping (Table S1), washed and fixed in 1% paraformaldehyde (PFA). Samples were acquired on BD LSRFortessa cell analyzer and the data were analyzed using FlowJo software v10.7.1 (FlowJo Inc).

Plasma cytokine and chemokine quantification by Luminex

Plasma cytokine and chemokine analysis at baseline, 24 hours and 14 days following the first dose were performed using ProcartaPlex NHP Cytokine & Chemokine Panel 30plex (Thermo Fisher) according to the manufacturer's instructions. Samples were analyzed using a MagPix (Luminex) instrument and the data were analyzed with BelysaTM Immunoassay Curve Fitting software (Millipore). Standard curves were generated using 5-parameter logistic (5-PL) curve fit.

Non human primate plasma ELISA assays

Recombinant proteins were acquired through the Global Health-Vaccine Accelerator Platform (GH-VAP) funded by the Bill & Melinda Gates Foundation, Seattle, WA, USA. Polyclonal antibody responses elicited in blood and BAL were analyzed using 96-well half area ELISA plates coated with recombinant antigens (SARS-CoV-2 prefusion (S-2P) stabilized S-protein (S), receptor binding domain (RBD), variant S-proteins (HexaPro Spike backbone) in PBS at 1 μg/mL overnight at 4ºC. Plates were washed three times with PBS containing 0.05% Tween-20 (PBS-T) and blocked with block buffer (PBS + 5% skim milk powder) for 1 hour at room temperature (RT). Samples were serially diluted in block buffer, added to the ELISA plate, and incubated for 2 hours at RT. For the RBD competition ELISA, samples were pre-incubated with or without 20 μg/mL RBD in block buffer for 30 min before being added to S-coated ELISA plate. For the chaotropic wash ELISA, plates were treated with 1.5 M NaSCN or PBS for 10 min at RT after sample incubation. Plates were washed three times and goat anti-monkey IgG-HRP (Nordic MUBio) in block buffer was added to the plate for 1 hour at RT. Plates were developed using 1-Step™ Ultra TMB-ELISA substrate (Thermo Fisher) and the reaction was stopped with 1 M H_2SO_4. The plates were read at 450 nm, with background correction at 550 nn. The data were analyzed with Prism 9.2.0 using 4-parameter logistic (4-PL) curve fit. Proportions of RBD-binding antibodies were determined from a decrease in ED_{50} when RBD was added as a competitor. The avidity index was calculated from the ratio of ED_{50} values between PBS and NaSCN conditions.

Monoclonal antibody ELISA assays

For monoclonal antibody (mAb) characterization, the ELISA was performed as above with the following modifications. Plates were coated with 4 μg/mL recombinant protein overnight at 4ºC, washed and blocked as described. Samples were serially diluted in block buffer and added to the ELISA plate. In the chaotropic wash ELISA, 1.0 M NaSCN or PBS were used to assess the strength of the binding interaction. After sample incubation for two hours, plates

were washed and goat anti-human IgG-HRP, Fc-specific (Jackson ImmunoResearch) in block buffer was added for 1 hour incubation. Plate development and data analysis were as described above.

Recombinant hACE2-human Fc fusion protein and previously characterized S-protein specific monoclonal antibodies were used as references: CR3022,[62] B38,[63] C144,[64] S309,[65] SM211,[66] S2X333,[67] and COVA2-37.[68]

Neutralization assays

Live virus neutralization assay was performed at Vismederi (Sienna, Italy) using SARS-CoV-2 2019-2019-nCoV strain 2019-nCov/Italy-INMI1 clinical isolate as described previously.[69] Briefly, serial twofold dilutions of heat-inactivated serum samples, starting at 1:10, were mixed with an equal volume of viral solution with 100 $TCID_{50}$ of SARS-CoV-2 and incubated for 1 hour before being transferred in duplicate to plates containing semi-confluent Vero E6 monolayers. The plates were incubated for four days at 37°C and 5% CO_2. After four days the plates were inspected using an inverted optical microscope. The highest serum dilution that protected more than 50% of cells from cytopathic effects was designated as the NT_{50}. The first WHO International Standard for anti-SARS-CoV-2 immunoglobulin (NIBSC 20/136) was analyzed in parallel to NHP samples for comparison.

Pseudovirus-particle neutralization assays

The pseudovirus-particle neutralization assay (PNA) was performed at Nexelis (Laval, Canada) using VSVΔG spike pseudotyped virus with a luciferase reporter as described previously.[70] Briefly, serial twofold dilution series of heat-inactivated serum were incubated with a constant amount of pseudotyped virus particles, and then transferred onto Vero E6 cells in 96-well plates. Test plates were incubated at 37°C and 5% CO_2 overnight. The next day, luciferase substrate was added to the plates which were read using a luminescence

493 microplate reader equipped with SoftMax Pro GxP software (v 6.5.1. or higher). The assay
494 was run in duplicate, and the serum dilution that neutralizes 50% of the pseudo-virus particles
495 (PNT_{50}) was interpolated by linear regression of the two serum dilution flanking 50% of the
496 control luminescene signal.

497 ***Electrochemiluminescence-based spike antigen detection***

498 SARS-CoV-2 spike antigen was quantified using the S-PLEX SARS-CoV-2 spike Kit
499 (K150ADJS, Meso Scale Diagnostics, Maryland, USA) according to manufacturer
500 instructions at the SciLifeLab Affinity Proteomics unit (Uppsala, Sweden). For the analysis,
501 25 µl sample was used and the plates were read using a MESO QuickPlex SQ 120
502 instrument. An 8-point calibration standard curve, based on recombinant SARS-CoV-2
503 protein included in the kit, was used to convert raw signals into data expressed in fg/ml.

504 ***T cell stimulation***

505 To assess the frequency of S-protein-specific memory T cells in blood and BAL, T cell re-
506 stimulation with overlapping peptides was performed as previously described.[10] Briefly, 1.5 x
507 10^6 PBMCs or BAL cells were cultured in 0.2 mL complete media (RPMI 1640
508 supplemented with 10% heat-inactivated FCS, 100 U/mL penicillin, 100 µg/mL
509 streptomycin, and 2 mM L-glutamine) in a 96-well plate at 37ºC, 5% CO_2. The cells were
510 stimulated with 2 µg/mL PepMix™ SARS-CoV-2 overlapping peptide library in DMSO
511 (15mers with 11 amino acid overlap, JPT Peptide Technologies), spanning the whole Spike
512 protein, or equal volume of DMSO only, in the presence of 10 µg/mL Brefeldin A (Life
513 Technologies). Following overnight stimulation, cells were stained with Live/Dead™ Fixable
514 Blue Dye (Life technologies), surface stained, fixed and permeabilized with
515 Cytofix/Cytoperm kit (BD) and stained intracellularly with the panel of antibodies listed in
516 Table S2. Cells were washed after staining and fixed with 1% PFA. Samples were acquired

on BD LSRFortessa cell analyzer and the data were analyzed using FlowJo software v10.7.1 (FlowJo Inc). DMSO-stimulated cells were used for background subtraction.

Spike-protein-specific memory B cell quantification and sorting

Recombinant SARS-CoV-2 prefusion stabilized S-protein and RBD were biotinylated using an EZ-Link® Micro Sulfo-NHS-LC Biotinylation Kit (Thermo Fisher) according to the manufacturer's instructions. Probes were generated by coupling biotinylated proteins to fluorophore-conjugated streptavidin (SA) molecules for detection by flow cytometry (SA-BV421, SA-APC and SA-PE, Biolegend). Isolated PBMCs were stained by a panel of antibodies listed in Table S3, as well as S-protein and RBD probes (S-APC, S-PE and RBD-BV421, 100 ng each). The samples were analyzed on a BD Aria III Fusion cell sorter (weeks 6 and 30) or a BD LSRFortessa flow cytometer (all other timepoints). At weeks 6 and 30, memory B cells (CD3- CD11c- CD14- CD16- CD123- HLA-DR+ CD20+ IgM- IgG+), double-positive for S-protein-binding, were single-cell sorted into 96-well plates and frozen immediately on dry ice for subsequent BCR amplification. Data were analyzed using FlowJo v10.7.1 (FlowJo Inc).

Single cell VDJ amplification and Sanger sequencing

RNA extraction and reverse-transcription using random hexamers from single-cell sorted S-protein-specific memory B cells were performed using the Superscript III Reverse transcriptase (Invitrogen) according to the manufacturer's instructions. Nested PCR was performed using reagents and procedures as previously reported for heavy and light immunoglobulin chains.[71] PCR products were Sanger sequenced by Genewiz (Leipzig, Germany), and resulting sequences were aligned to the Karolinska Macaque database KIMDB (1.0)[72] using IgDiscover.[73]

Sequence data analysis and monoclonal antibody selection

Clonally-related sequences were identified using heavy chain sequences and Clonotypes module of IgDiscover,[73,74] applying established criteria to define a clone – same V and J gene assignment, same CDRH3 length, 80% similarity in CDRH3 and one identical CDRH3 junction.[32] Several lineages were detected at both week 6 and week 30, and respective antibody sequences were selected for mAb expression and characterization. Cloning, expression, and purification of mAbs as human IgG1 in mammalian cells were performed by Genscript (Leiden, Netherlands).

Antigen-specific antibody-secreting cell detection in blood

Antigen-specific plasmablasts were enumerated by enzyme-linked immunospot (ELISpot) on the day of the booster dose and four days after. Multiscreen IP filter ELISpot 96-well plates (Millipore) were activated with 35% ethanol for 1 minute and washed three times with PBS. Plates were coated overnight with 1 μg/mL Affinity Pure Goat Anti-Human IgG, Fc fragment-specific antibody (Jackson ImmunoResearch). The next day, plates were washed three times with PBS and blocked with complete media for 1.5 hours. Serially diluted, freshly isolated PBMCs were incubated overnight at 37ºC, 5% CO_2. After incubation, plates were washed six times with PBS-T (0.05%) and incubated with biotinylated probes for 1.5 hours: 0.25 μg/mL goat anti-human IgG Fc fragment specific (Jackson ImmunoResearch), 1 μg/mL prefusion stabilized S-protein, 1 μg/mL RBD or 1 μg/mL ovalbumin, to detect total IgG and antigen-specific IgG producing cells, respectively. The plates were washed six times with PBS-T and incubated with 1:1000 diluted SA-conjugated alkaline phosphatase (Mabtech AB) for 30 minutes. After another round of washing, plates were developed with nitro-blue tetrazolium 5-bromo-4-chloro-3′indolyphosphate (BCIP/NBT) precipitating substrate (Mabtech AB) for 5 minutes. An AID ELISpot reader (Autoimmun Diagnostika) was used to obtain spot counts. Ovalbumin wells were used for background-subtraction.

In vitro uptake and translation of mCitrine LNP/mRNA

Primary human monocytes were isolated from buffy coats using RosetteSep™ Human Monocyte Enrichment Cocktail (Stemcell Technologies) and gradient density centrifugation using Ficoll-Pacque (GE Healthcare) according to manufacturer's instructions. After isolation, $1.5x10^6$ monocytes were cultured in 0.5 mL complete media (RPMI 1640 supplemented with 10% heat-inactivated FCS, 100 U/mL penicillin, 100 µg/mL streptomycin, and 2 mM L-glutamine) at 37ºC and 5% CO_2, in the presence of mCitrine-encoding mRNA in DiD-labelled lipid nanoparticles at different mRNA concentrations (0.0 – 5.0 µg/mL) for an indicated amount of time (6–72 hours). After culture, cells were washed with PBS, stained with Live/Dead™ Fixable Blue Dye (Life technologies) and FcR blocking reagent (Miltenyi Biotec), followed by surface staining with the panel of antibodies listed in Table S4. Cells were then washed with PBS and fixed with 1% PFA. Samples were acquired on BD LSRFortessa cell analyzer and the data were analyzed using FlowJo software v10.7.1 (FlowJo Inc).

Biodistribution immunizations and sample collection

To study the innate immune responses to different mRNA doses, rhesus macaques received four i.m. doses into marked injection sites, one in each limb. Vaccines (0.5 mL/injection) contained either saline as control, 10 or 100 µg mCitrine-encoding mRNA in DiD-labelled lipid nanoparticles. Site of injection as well as vaccine-draining and non-draining tissues were sampled at necropsy 24 hours after immunization, and stored in RPMI 1640 on ice as previously described.[35,75]

Biodistribution experiments sample processing

Muscle biopsies were dissected and weighed before digestion into single cell suspensions as previously described.[35,75] Briefly, muscle tissue was incubated at 37°C for 2 hours without agitation in the presence of 0.25 mg/mL Liberase TL (Roche) and 0.5 mg/mL DNase I

(Sigma). Enzyme activity was quenched by addition of complete media, the mixtures were filtered through 70 μm cell strainers twice and single cell suspensions were washed before proceeding to the next step. Liver and bone marrow samples were processed by standard gradient density centrifugation, in the same manner as blood samples. Lymphoid tissues were mechanically disrupted using a plunger and a 70 μm cell strainer, and washed with complete media. Once sample processing was complete, single cell suspensions were immediately stained for flow cytometry analyses.

Biodistribution experiments flow cytometry

To quantify mCitrine-vaccine signal in different immune cell populations, cell suspensions corresponding to approximately 2 g of muscle tissue or 5 million lymph node cells were stained for flow cytometry. First, cells were stained with Live/Dead™ Fixable Blue Dye (Life technologies) and FcR blocking reagent (Miltenyi Biotec), followed by a panel of antibodies listed in Table S4. Samples were then washed and fixed with 1% PFA. Before acquisition, AccuCount beads (Spherotech) were added to each sample for quantification according to the manufacturer's instructions. Samples were acquired on a BD LSRFortessa flow cytometer cell analyzer and the data were analyzed using FlowJo v10.7.1 (FlowJo Inc).

Statistics

No statistical methods were used to predetermine sample size. The results were considered statistically significant when $p < 0.05$. For comparison of two groups of paired and unpaired samples, non-parametric Wilcoxon matched-pairs signed rank test and Mann-Whitney U test were used, respectively. For comparison of three of more groups, the non-parametric Kruskal-Wallis test with Dunn's multiple comparison test was used. Correlations were assessed using non-parametric Spearman's correlation. Analyses were performed in GraphPad Prism 9.

DATA AVAILABILITY STATEMENT

BCR sequencing data has been deposited to GenBank under accession numbers OP572523: OP573208.

AUTHOR CONTRIBUTIONS

Conceptualization – K.Le., K.S., B.P., K.Lo.; Formal Analysis – K.Le., R.A.C., K.Lo.; Funding acquisition – B. P., K. Lo.; Investigation – K. Le., F.H., S.O., X.Y., A.C., R.A.C., I.W., J.H.; Methodology – K.Le., F.H., S.O.; Resources – S.O.M., E.J., K.S., S.R., B.P., K.Lo.; Supervision – K. Lo.; Visualization – K.Le.; Writing – original draft – K.Le, K.Lo.; Writing – review & editing – all authors.

ACKNOWLEDGEMENTS

We would like to thank the team from Affinity Proteomics-Stockholm at SciLifeLab Sweden for technical support and the generation of systemic cytokine data for this project. We would like to acknowledge support of Affinity Proteomics-Uppsala at SciLifeLab Sweden for providing assistance in protein analyses. We would like to thank Lauren Carter and the Nanoparticle Core Laboratory at the University of Washington Institute for Protein Design for protein reagents, and Holger Kanzler from the Bill & Melinda Gates Foundation for inputs and insights throughout the study. Keith Veitch (keithveitch communications, Amsterdam, the Netherlands) and Margaret Haugh (CureVac) provided editorial support for the manuscript. This work was supported by grants from the Bill & Melinda Gates Foundation (OPP1192908 and INV-017217 to K.Lo), Swedish Research Council (2019-01036 and 2020-05829 to K.Lo.), the Knut and Alice Wallenberg Foundation through SciLifeLab and Karolinska Institutet (VC-2021-0017 to K.Lo), and Coalition for Epidemic Preparedness Innovations (CEPI, RRCU2001 to CureVac AG). Also, this research was

637 supported by intramural faculty salary grants from Karolinska Institutet (K.Le., F.H, and S.O)
638 and a grant from the China Scholarship Council (X.Y.).

639 **DECLARATION OF INTERESTS STATEMENT**

640 S.O.M, E.J., K.S., S.R. and B.P.are employees of CureVac AG.

641 **KEYWORDS**

642 Vaccine, mRNA vaccine, antibody response, vaccine biodistribution, innate immunity,
643 COVID-19, SARS-CoV-2.

REFERENCES

1. COVID19 vaccine tracker. Available online at https://covid19.trackvaccines.org/ Accessed June 13 2022.

2. Kremsner, P.G., Guerrero, R.A.A., Arana-Arri, E., Martine, G.J.A., Bonten, M., Chandler, R., Corra, G., De Block, E.J.L., Ecke, L., Gabo, J.J., et al. (2022) Efficacy and safety of the CVnCoV SARS-CoV-2 mRNA vaccine candidate in ten countries in Europe and Latin America (HERALD): a randomised, observer-blinded, placebo-controlled, phase 2b/3 trial. Lancet Infect. Dis. *22*, 329–340.

3. Polack, F.P., Thomas, S,J,, Kitchin, N., Absalon, J., Gurtman, A., Lockhart, S., Perez, J.L., Marc, G.P., Moreira, E.D., Zerbini, C., et al. (2020) Safety and efficacy of the BNT162b2 mRNA COVID-19 vaccine. N Engl J Med *383*, 2603–2615.

4. Baden, L.R., El Sahly, H.M., Essink, B., Kotloff, K., Frey, S., Novak, R., Diemert, D., Spector, S.A., Rouphael, N., Creech, C.B, et al. (2021) Efficacy and safety of the mRNA-1273 SARS-CoV-2 vaccine. N Engl J Med *384*, 403–416.

5. Kremsner, P.G., Mann, P., Kroidl, A., Leroux-Roels, I., Schindler, C., Gabor, J.J., Schunk, M., Leroux-Roels, G., Bosch, J.J., Fendel, R., et al. (2021) Safety and immunogenicity of an mRNA-lipid nanoparticle vaccine candidate against SARS-CoV-2. Wiener klinische Wochenschrift *133*, 931–941.

6. Gebre, M.S., Rauch, R., Roth, N., Yu, J., Chandrashekar, A., Mercado, N.B., He, X., Liu, J., McMahan, K., Martinot, A., et al. (2022) Optimization of non-coding regions for a non-modified mRNA COVID-19 vaccine. Nature *601*, 410–414.

7. Rauch, S., Gooch, K., Hall, Y., Salguero, F.J., Dennis, M.J., Gleeson, F.V., Harris, D., Ho, C., Humphries, H.E., Longet, S., et al. (2020) mRNA vaccine CVnCoV protects non-human primates from SARS-CoV-2 challenge infection. bioRxiv doi: https://doi.org/10.1101/2020.12.23.424138

8. van Doremalen, N., Fische, R.J., Schulz, J.E., Holbrook, M.G., Smith, B.J., Lovaglio, J., Petsch, B., and Munster, V.J. (2021) Immunogenicity of low-dose prime-boost vaccination of mRNA vaccine CV07050101 in non-human primates. Viruses *13*, 1645.

9. Kwissa, M., Nakaya, H.I., Oluoch, H., and Pulendran, B. (2012) Distinct TLR adjuvants differentially stimulate systemic and local innate immune responses in nonhuman primates. Blood *119*, 2044–2055.

10. Thompson, E.A., Ols, S., Miura, K., Rausch, K., Narum, D.L., Spångberg, M., Juraska, M., Wille-Reece, U., Weiner, A., Howard, R.F., et al. (2018) TLR-adjuvanted nanoparticle vaccines differentially influence the quality and longevity of responses to malaria antigen Pfs25. JCI Insight *3*, e120692.

11. Arunachalam, P.S., Scott, M.K.D., Hagan, T., Li, C., Feng, Y., Wimmers, F., Grigoryan, L., Trisal, M., Edara, V.V., Lai, L., et al. (2021) Systems vaccinology of the BNT162b2 mRNA vaccine in humans. Nature *596*, 410–416.

12. Wolz, O.-O., Kays, S.-K., Junker, H., Koch, S.D., Mann, P., Quintini, G., von Eisenhart-Rothe, P. and Oostvogels, L. (2022) A third dose of the COVID-19 vaccine, CVnCoV, increased the neutralizing activity against the SARS-CoV-2 wild-type and Delta variant. Vaccines (Basel). *10*, 508.

13. Garcia-Beltran, W.F., St Denis, K.J,, Hoelzemer, A., Lam, E.C., Nitido, A.D., Sheehan, M.L., Berrios, C, Ofoman, O., Chang, C.C., Hauser, B.M, et al. (2022) mRNA-based COVID-19 vaccine boosters induce neutralizing immunity against SARS-CoV-2 Omicron variant. Cell *185*, 457–466.

14. Falsey, A.R., Frenck Jr, R.W., Walsh, E.E., Kitchin, N., Absalon, J., Gurtman, A., Lockhart, S., Bailey, R., Swanson, K.A., Xu, X., et al (2021) SARS-CoV-2 neutralization with BNT162b2 vaccine dose 3. N Engl J Med *385*, 1627–1629.

15. Wratil, P.R., Stern, M., Priller, A., Willmann, A., Almanzar, G., Vogel, E., Feuerherd, M., Cheng, C-C., Yazici, S., Christa, C., et al. (2022) Three exposures to the spike protein of SARS-CoV-2 by either infection or vaccination elicit superior neutralizing immunity to all variants of concern. Nat Med *28*, 496–503.

16. Röltgen, K., Nielsen, S.C.A., Silva, O., Younes, S.F., Zaslavsky, M., Costales, C., Yang, F., Wirz, O.F., Solis, D., Hoh, R.A., et al. (2022) Immune imprinting, breadth of variant recognition, and germinal center response in human SARS-CoV-2 infection and vaccination. Cell *185*, 1025–1040.

17. Corbett, K.S., Flynn, B., Foulds, K.E., Francica, J.R., Boyoglu-Barnum, S., Werner, A.P., Flach, B., O'Connell, S., Bock, K.W., Minai, M., et al. (2020) Evaluation of the mRNA-1273 vaccine against SARS-CoV-2 in nonhuman primates. N Engl J Med *383*, 1544–1555.

18. Vogel, A.B., Kanevsky, I., Che, Y., Swanson, K.A., Muik, A., Vormehr, M., Kranz, L.M., Walzer, K.C., Hein, S., Güler, A., et al. (2021) BNT162b vaccines protect rhesus macaques from SARS-CoV-2. Nature *592*, 283–289.

19. Widge, A.T., Rouphael, N.G., Jackson, L.A., Anderson, E.J., Roberts, P.C., Makhene, M., Chappell, J.D., Denison, M.R., Stevens, L.J., Pruijssers, A.J., et al. (2021) Durability of responses after SARS-CoV-2 mRNA-1273 vaccination. N Engl J Med *384*, 80–82.

20. Sahin, U., Muik, A., Derhovanessian, E., Vogler, I., Kranz, L.M., Vormehr, M., Baum, A., Pascal, K., Quandt, J., Maurus, D., et al. (2020) COVID-19 vaccine BNT162b1 elicits human antibody and T_H1 T cell responses. Nature *586*, 594–599.

21. Corbett, K.S., Nason, M.C., Flach, B., Gagne, M., O'Connell, S., Johnston, T.S., Shah, S.N., Edara, V.V., Floyd, K., Lai, L., McDanal, C., et al (2021) Immune correlates of protection by mRNA-1273 vaccine against SARS-CoV-2 in nonhuman primates. Science *373*; eabj0299.

22. Khoury, D.S., Cromer, D., Reynaldi ,A., Schlub, T.E., Wheatley, A.K., Juno, J.A., Subbarao, K., Kent, S.J., Triccas, J.A., and Davenport, M,P. (2021) Neutralizing antibody levels are highly predictive of immune protection from symptomatic SARS-CoV-2 infection. Nat Med *27*, 1205–1211.

23. Cromer, D., Steain, M., Reynaldi, A., Schlub, T.E., Wheatley, A.K., Juno, J.A, Kent, S.J., Triccas, J.A., Khour, D.S., and Davenport, M.P. (2022) Neutralising antibody titres as predictors of protection against SARS-CoV-2 variants and the impact of boosting: a meta-analysis. Lancet Microbe *3*, e52–e61.

24. Goel, R.R., Painter, M.M., Apostolidis, S.A., Mathew, D., Meng, W., Rosenfeld, A.M., Lundgreen, K.A., Reynaldi, A., Khoury, D.S., Pattekar, A., et al. (2021) mRNA vaccines induce durable immune memory to SARS-CoV-2 and variants of concern. Science *374*, abm0829.

25. Cagigi, A., Yu, M, Österberg, B., Svensson, J., Falck-Jones, S., Vangeti, S., Åhlberg, E., Azizmohammadi, L., Warnqvist, A., Falck-Jones, R. et al. (2021) Airway antibodies emerge according to COVID-19 severity and wane rapidly but reappear after SARS-CoV-2 vaccination. JCI Insight 6, e151463.

26. Lederer, K., Bettini, E., Parvathaneni, K., Painter, M.M., Agarwal, D., Lundgreen, K.A., Weirick, M., Muralidharan, K., Castaño, D., Goel, R.R., et al. (2022) Germinal center responses to SARS-CoV-2 mRNA vaccines in healthy and immunocompromised individuals. Cell *185*, 1008–1024.

27. Byrnes, J.R., Zhou, X.X., Lui, I., Elledge, S.K., Glasgow, J.E., Lim, S.A., Loudermilk, R.P., Chiu, C.Y., Wang, T.T., Wilson, M.R., et al. (2020) Competitive SARS-CoV-2 serology reveals most antibodies targeting the spike receptor-binding domain compete for ACE2 binding. mSphere *5*, e00802-20.

28. Bernat, N.V., Corcoran, M., Nowak, I., Kaduk, M., Dopico, X.C., Narang, S., Maisonasse, P., Dereuddre-Bosquet, N., Murrell, B., Hedestam, G.B.K. (2021) Rhesus and cynomolgus macaque immunoglobulin heavy-chain genotyping yields comprehensive databases of germline VDJ alleles. Immunity *54*, 355–366.e4.

29. Kim, W., Zhou J.Q., Horvath, S.C., Schmitz, A.J., Sturtz, A.J., Lei, T., Liu, Z., Kalaidina, E., Thapa, M., Alsoussi, W.B. et al. (2022) Germinal centre-driven maturation of B cell response to mRNA vaccination. Nature *604*, 141–145.

30. Dejnirattisai, W., Zhou, D., Ginn, H.M., Duyvesteyn, H.M.E., Supasa, P., Case, J.B., Zhao, Y., Walter , T.S., Mentzer, A.J., Liu, C., et al. (2021) The antigenic anatomy of SARS-CoV-2 receptor binding domain. Cell *184*, 2183–2200.

31. Goel, R.R., Painter, M.M., Lundgree, K.A., Apostolidis, S.A., Baxter, A.E., Giles, J.R., Mathew, D., Pattekar, A., Reynaldi, A., Khoury, D.S., et al. (2022) Efficient recall of Omicron-reactive B cell memory after a third dose of SARS-CoV-2 mRNA vaccine. Cell *185*, P1875–1887.

32. Liang, F., Lindgren, G., Lin, A., Thompson, E.A., Ols, S., Röhss, J., John, S., Hassett, K., Yuzhakov, O., Bahl, K., et al. (2017) Efficient targeting and activation of antigen-presenting cells in vivo after modified mRNA vaccine administration in Rhesus macaques. Mol Ther *25*, 2635–2647.

33. Lindsay, K.E., Bhosle, S.M., Zurla, C., Beyersdorf, J., Rogers, K.A., Vanover, D., Xiao, P., Araínga, M., Shirreff, L.M., Pitard, B., et al. (2019) Visualization of early events in mRNA vaccine delivery in non-human primates via PET-CT and near-infrared imaging. Nat Biomed Eng *3*, 371–380.

34. Liang, F., Lindgren, G., Sandgren, K.J., Thompson, E.A., Francica, J.R., Seubert, A., De Gregorio, E., Barnett, S., O'Hagan, D.T., Sullivan, N.J., et al. (2017) Vaccine priming is restricted to draining lymph nodes and controlled by adjuvant-mediated antigen uptake. Science Trans Med *9*, eaal2094.

35. Ols, S., Yang, L., Thompson, E.A., Pushparaj, P., Tran, K., Liang, F., Lin, A., Eriksson, B., Hedestam, G.B.K., Wyatt, R.T., et al. (2020) Route of vaccine administration alters antigen trafficking but not innate or adaptive immunity. Cell Rep *30*, 3964–3971.e7.

36. Munro, A.P.S., Janani, L., Cornelius, V., Aley, P.K., Babbage, G., Baxter, D., Bula, M., Cathie, K., Chatterjee, K., Dodd, K., et al. (2021) Safety and immunogenicity of seven COVID-19 vaccines as a third dose (booster) following two doses of ChAdOx1 nCov-19 or BNT162b2 in the UK (COV-BOOST): a blinded, multicentre, randomised, controlled, phase 2 trial. Lancet 398, 2258–2276.

37. Harvey, W.T., Carabelli, A.M., Jackson, B., Gupta, R.K., Thomson, E.C., Harrison, E. M., Ludden, C., Reeve, R., Rambaut, A., Peacock, S.J., et al. (2021) SARS-CoV-2 variants, spike mutations and immune escape. Nat Rev Microbiol 19, 409–424.

38. Gagne M, Corbett KS, Flynn BJ, Foulds KE, Wagner DA, Andrew SF, Todd JM, Honeycutt CC, McCormick L, Nurmukhambetova ST, et al. (2022) Protection from SARS-CoV-2 Delta one year after mRNA-1273 vaccination in rhesus macaques coincides with anamnestic antibody response in the lung. Cell *185*, 113-130.

39. Alberer, M., Gnad-Vogt, U., Hong, H.S., Mehr, K.T., Backert, L., Finak, G., Gottardo, R., Bica, M.A., Garofan, A., Koch, S.D., et al. (2017) Safety and immunogenicity of a mRNA rabies vaccine in healthy adults: an open-label, non-randomised, prospective, first-in-human phase 1 clinical trial. Lancet *390*, 1511–1520.

40. Aldrich, C., Leroux-Roels, I., Huang, K.B., Bica, M.A., Loeliger, E., Schoenborn-Kellenberger, O., Walz, L., Leroux-Roels, G., von Sonnenburg, F., and Oostvogels, L. (2021) Proof-of-concept of a low-dose unmodified mRNA-based rabies vaccine formulated with lipid nanoparticles in human volunteers: A phase 1 trial. Vaccine *39*, 1310–1318.

41. Cagigi, A., and Loré, K. (2021) Immune responses induced by mRNA vaccination in mice, monkeys and humans. Vaccines (Basel) *9*, 61.

42. Lindgren, G., Ols, S., Liang, F., Thompson, E.A., Lin, A., Hellgren, F., Bahl, K., John, S., Yuzhakov, O., Hassett, K.J., Brito, L.A., et al. (2017) Induction of robust B cell responses after influenza mRNA vaccination is accompanied by circulating hemagglutinin-specific ICOS+ PD-1+ CXCR3+ T follicular helper cells. *Front Immunol 8*, 1539.

43. Gujer, C., Sandgren, K.J., Douagi, I., Adams, W.C., Sundling, C., Smed-Sörensen, A., Seder, R.A., Hedestam, G.B.K., and Loré, K.(2011) IFN-alpha produced by human plasmacytoid dendritic cells enhances T cell-dependent naive B cell differentiation. J Leukoc Biol *89*, 811–821.

44. Le Bon, A., Schiavoni, G., D'Agostino, G., Gresser, I., Belardelli, F., and Tough, D.F. (2001) Type i interferons potently enhance humoral immunity and can promote isotype switching by stimulating dendritic cells in vivo. Immunity *14*, 461–470.

45. Johnson, T.R., Rao, S., Seder, R.A., Chen, M., and Graham, B.S. (2009) TLR9 agonist, but not TLR7/8, functions as an adjuvant to diminish FI-RSV vaccine-enhanced disease, while either agonist used as therapy during primary RSV infection increases disease severity. Vaccine *27*, 3045–3052.

46. Francica, J.R., Sheng, Z., Zhang, Z., Nishimura, Y., Shingai, M., Ramesh, A., Keele, B.F., Schmidt, S.D., Flynn, B.J., Darko, S., et al. (2015) Analysis of immunoglobulin transcripts and hypermutation following SHIV(AD8) infection and protein-plus-adjuvant immunization. Nat Commun *6*, 6565.

47. Shah, J.A., Darrah, P.A., Ambrozak, D.R., Turon, T.N., Mendez, S., Kirman, J., Wu, C-Y., Glaichenhaus, N., and Seder, R.A. (2003) Dendritic cells are responsible for the capacity of CpG oligodeoxynucleotides to act as an adjuvant for protective vaccine immunity against Leishmania major in mice. et al., J Exp Med *198*, 281–291.

48. Tewari, K., Flynn, B.J., Boscardin, S.B., Kastenmueller, K., Salazar, A.M., Anderson, C.A., Soundarapandian, V., Ahumada, A., Keler, T., Hoffman, S.L., et al. (2010) Poly(I:C) is an effective adjuvant for antibody and multi-functional CD4+ T cell responses to Plasmodium falciparum circumsporozoite protein (CSP) and αDEC-CSP in non human primates. Vaccine *28*, 7256–7566.

49. Bergamaschi, C., Terpos, E., Rosati, M., Angel, M., Bear, J., Stellas, D., Karaliota, S., Apostolakou, F., Bagratuni, T., Patseas, D., et al (2021) Systemic IL-15, IFN-γ, and IP-

10/CXCL10 signature associated with effective immune response to SARS-CoV-2 in BNT162b2 mRNA vaccine recipients. Cell Rep *36*, 109504.

50. Jakubzick, C.V., Randolph, G.J. and Henson, P.M. (2017) Monocyte differentiation and antigen-presenting functions. Nat Rev Immunol *17*, 349–362.

51. Kwissa, M., Nakaya, H.I., Onlamoon, N., Wrammert, J., Villinger, F., Perng, G.C., Yoksan, S., Pattanapanyasat, K., Chokephaibulkit, K., Ahmed, R., et al. (2014) Dengue virus infection induces expansion of a CD14(+)CD16(+) monocyte population that stimulates plasmablast differentiation. Cell Host Microbe *16*, 115–127.

52. Zhu, H., Hu, F., Sun, X., Zhang, X., Zhu, L., Liu, X., Li, X., Xu, L., Shi, L., Gan, Y., et al. (2016) CD16 + monocyte subset was enriched and functionally exacerbated in driving T-cell activation and B-cell response in systemic lupus erythematosus. Front Immunol *7*, 512.

53. Glaros, V., Rauschmeier, R., Artemov, A.V., Reinhardt, A., Ols, S., Emmanouilidi, A., Gustafsson, C., You, Y., Mirabello, C., Björklund , A.K., et al. (2021) Limited access to antigen drives generation of early B cell memory while restraining the plasmablast response. Immunity *54*, 2005–2023.

54. Voss, W.N., Hou, Y.J., Johnson, N.V., Delidakis, G., Kim, J.E., Javanmardi, K., Horton, A.P., Bartzoka, F., Paresi, C.J., Tanno, Y., et al. (2021) Prevalent, protective, and convergent IgG recognition of SARS-CoV-2 non-RBD spike epitopes. Science *372*, 1108–1112.

55. Amanat, F., Thapa, M., Lei, T., Ahmed, S.M.S., Adelsberg, D.C., Carreño, J.M., Strohmeier, S., Schmitz, A.J., Zafar, S., Zhou, J.Q., et al. (2021) SARS-CoV-2 mRNA vaccination induces functionally diverse antibodies to NTD, RBD, and S2. Cell *184*, 3936–3948.e10.

56. Beaudoin-Bussières, G., Chen, Y., Ullah, I., Prévost, J., Tolbert, W.D., Symmes, K., Ding, S., Benlarbi, M., Gong, S.Y., Tauzin, A., et al. (2022) A Fc-enhanced NTD-binding non-neutralizing antibody delays virus spread and synergizes with a nAb to protect mice from lethal SARS-CoV-2 infection. Cell Rep *38*, 110368.

57. Bahnan, W., Wrighton, S., Sundwall, M., Bläckberg, A., Larsson, O., Höglund, U., Khakzad, H., Godzwon, M., Walle, M., Elder, E., et al. (2022) Spike-dependent opsonization indicates both dose-dependent inhibition of phagocytosis and that non-

neutralizing antibodies can confer protection to SARS-CoV-2. Front Immunol. *12*, 808932.

58. Feng, S., Phillips, D.J., White, T., Sayal, H., Aley, P.K., Bibi, S., Dold, C., Fuskova, M., Gilbert, S.C., Hirsch, I., et al. (2021) Correlates of protection against symptomatic and asymptomatic SARS-CoV-2 infection. Nat Med *27*, 2032–2040.

59. Goel, R.R., Painter, M.M., Lundgreen, K.A., Apostolidis, S.A., Baxter, A.E., Giles, J.R., Mathew, D., Pattekar, A., Reynaldi, A., Khoury, D.S., et al. (2022) Efficient recall of Omicron-reactive B cell memory after a third dose of SARS-CoV-2 mRNA vaccine. Cell *185*, 1875-1887.e8.

60. Sáez-Llorens, X., Lanata, C., Aranguren, E., Celis, C.R., Cornejo, R., DeAntonio, R., Ecker, L., Garrido, D., Gil, A.I., Gonzales, M., et al. (2022) Safety and immunogenicity of mRNA-LNP COVID-19 vaccine CVnCoV in Latin American adults: a phase 2 randomized study. Vaccine X In press https://doi.org/10.1016/j.jvacx.2022.100189.

61. Griesbeck, O., Baird, G.S., Campbell, R.E., Zacharias, D.A., and Tsien, R.Y. (2001) Reducing the environmental sensitivity of yellow fluorescent protein. J Biol Chem *276*, 29188–29194.

62. Yuan, M., Wu, N.C., Zhu, X., Lee, C.-C.D., So, R.T.Y., Lv, H., Mok, C.K.P., and Wilson, I.A. (2020) A highly conserved cryptic epitope in the receptor binding domains of SARS-CoV-2 and SARS-CoV. Science *368*, 630–633.

63. Wu, Y., Wang, F., Shen, C., Peng, W., Li, D., Zhao, C., Li, Z., Li, S., Bi, Y., Yang Y., et al. (2020) A noncompeting pair of human neutralizing antibodies block COVID-19 virus binding to its receptor ACE2. Science *368*, 1274–1278.

64. Robbiani, D.F., Gaebler, C., Muecksch, F., Lorenzi, J.C.C., Wang, Z., Cho, A., Agudelo, M., Barnes, C.O., Gazumyan, A., Finkin, S., et al. (2020) Convergent antibody responses to SARS-CoV-2 in convalescent individuals. Nature *584*, 437–442.

65. Pinto, D., Park, Y.-J., Beltramello, M., Walls, A.C., Tortorici, M.A., Bianchi, S., Jaconi, S., Culap, K., Zatta, F., De Marco, A., et al. (2020) Cross-neutralization of SARS-CoV-2 by a human monoclonal SARS-CoV antibody. Nature *583*, 290–295.

66. Tortorici, M.A., Beltramello, M., Lempp, F.A., Pinto, D., Dang, H.V., Rosen, L.E., McCallum, M., Bowen, J., Minola, A., Jaconi, S., et al. (2020) Ultrapotent human

887 antibodies protect against SARS-CoV-2 challenge via multiple mechanisms. Science
888 *370*, 950–957.

889 67. McCallum, M., De Marco, A., Lempp, F.A., Tortorici, M.A., Pinto, D., Walls, A.C.,
890 Beltramello, M., Chen, A., Liu, Z., Zatta, F., et al. (2021) N-terminal domain antigenic
891 mapping reveals a site of vulnerability for SARS-CoV-2. Cell *184*, 2332–2347.

892 68. Brouwer, P.J.M., Caniels, T.G., van der Straten, K., Snitselaar, J.L., Aldon, Y.,
893 Bangaru, S., Torres, J.L., Okba, N.M.A., Claireaux, M., Kerster, G., et al (2020) Potent
894 neutralizing antibodies from COVID-19 patients define multiple targets of
895 vulnerability. Science *369*, 643–650.

896 69. Manenti, A., Maggetti, M., Casa, E., Martinuzzi, D., Torelli, A., Trombetta, C.M.,
897 Marchi, S., and Montomoli, E. (2020) Evaluation of SARS-CoV-2 neutralizing
898 antibodies using a CPE-based colorimetric live virus micro-neutralization assay in
899 human serum samples. J Med Virol *92*, 2096–2104.

900 70. Bewley, K.R., Coombes, N.S., Gagnon, L., McInroy, L., Baker, N., Shaik, I., St-Jean,
901 J.R., St-Amant, N., Buttigieg, K.R., Humphries, H.E., et al. (2021) Quantification of
902 SARS-CoV-2 neutralizing antibody by wild-type plaque reduction neutralization,
903 microneutralization and pseudotyped virus neutralization assays. Nat Protoc *16*, 3114–
904 3140.

905 71. Sundling, C., Phad, G., Douagi, I., Navis, M., and Hedestam, G.B.K. (2012) Isolation
906 of antibody V(D)J sequences from single cell sorted rhesus macaque B cells. J
907 Immunol Methods *386*, 85–93.

908 72. Bernat, N.V., Corcora, M., Nowak, I., Kaduk, M., Dopico, X.C., Narang, S.,
909 Maisonasse, P., Dereuddre-Bosquet, N., Murrell, B, and Hedestam, G.B.K. (2021)
910 Rhesus and cynomolgus macaque immunoglobulin heavy-chain genotyping yields
911 comprehensive databases of germline VDJ alleles. Immunity *54*, 355-366.e4.

912 73. Corcoran, M.M., Phad, G.E., Bernat, N.V., Stahl-Hennig, C., Sumida, N., Persson,
913 M.A.A., Martin, M., and Hedestam, G.B.K. (2016) Production of individualized V gene
914 databases reveals high levels of immunoglobulin genetic diversity. Nat Commun *7*,
915 13642.

916 74. Phad, G.E., Pushparaj, P., Tran, K., Dubrovskaya, V., Àdori, M., Martinez-Murillo, P.,
917 Bernat, N.V., Singh, S., Dionne, G., O'Dell, S., et al. (2020) Extensive dissemination

and intraclonal maturation of HIV Env vaccine-induced B cell responses. J Exp Med *217*, e20191155.

75. Li, D., Edwards, R.J., Manne, K., Martinez, D.R., Schäfer, A., Alam, S.M., Wiehe, K., Lu, X., Parks, R., Sutherland, L.L., et al. (2021) In vitro and in vivo functions of SARS-CoV-2 infection-enhancing and neutralizing antibodies. Cell *184*, 4203–4219.e32.

924 **FIGURE LEGENDS**

925 **Figure 1: Innate immune response after mRNA immunization.** (A) Study design. (B)
926 Gating strategy used in immunophenotyping. (C, D) Total monocyte and monocyte subset
927 frequency in blood after immunization. (E) Plasma cytokines after immunization assessed by
928 30-plex Luminex assay. (F) Selected plasma cytokines after prime immunization (related to
929 type I interferon response, TNF and IL-6 as controls). (G) Principal component analysis of
930 plasma cytokines (30-plex assay). Figures C and D combine data from 3 NHPs after first and
931 3third immunizations. Figures E-G focus on the innate immune response after prime
932 immunization.

933

934 **Figure 2: Enhanced adaptive immune responses after the third dose.** (A) Plasma binding
935 antibody response to ancestral S-protein (S-2P) and RBD by ELISA. (B) Live virus
936 neutralization (NT50) in serum. Gray shaded area represents the neutralization titer of the
937 WHO International Standard (NIBSC 20/136). (C) VSV-based pseudovirus neutralization
938 (PNT_{50}) in serum. (D) Antibody neutralization potency index representing the ratio between
939 neutralizing (NT_{50}) and binding (ED_{50}) antibody titers in plasma. Data points following
940 second (weeks 6, 8 and 12) and third immunizations (weeks 30, 32, 35) are shown,
941 respectively. (E) S protein concentration in serum after first and third immunizations. (F, G)
942 Plasma antibody binding to variant S-proteins, and ratio between varinat and ancestral
943 binding titers. (H, I). Ancestral S-protein and RBD binding (H) and neutralizing antibodies
944 (I) in BAL. PP = Pre-pandemic BAL samples. (J) Correlation of plasma and BAL anti-S-
945 protein antibody titers. (K, L) Vaccine-specific plasmablasts in blood (K) and vaccine-
946 specific plasma cells in bone marrow (L) assessed using ELISpot. Representative wells are
947 shown on the right. Data is background subtracted based on OVA wells. ASC = antibody-
948 secreting cell. (M-O) Frequencies of S-protein-specific CD4 T helper cell subsets (M),

949 circulating T follicular cells (N) and CD8 T cells (O) in blood and BAL at selected
950 timepoints. All data is background subtracted based on DMSO-only condition. Significance
951 assessed by Wilcoxon signed-rank test, or Spearman correlation. Arrows indicate
952 immunizations. Dotted lines indicate limit of detection (LOD) of each assay, except panel F
953 where it represents the ratio of 1 (equal binding to ancestral and variant S protein). Data are
954 represented as mean ± SEM.

955

956 **Figure 3: Maturation of the B cell response after the third immunization.** (A)
957 Representative gates used for sorting S-protein-specific IgG+ memory B cells two weeks
958 after second and third immunizations (weeks 6 and 30). (B) Longitudinal assessment of S-
959 protein-specific memory B cells, out of IgG+ B cells. (C) Proportion of RBD-specific
960 memory B cells out of S-protein specific memory B cells at selected timepoints. (D)
961 Proportion of RBD-binding antibodies in serum at selected timepoints. (E) SHM in sorted
962 memory B cells, presented as number of nucleotide substitutions in the heavy chain V gene
963 segment. (F) Avidity index of a polyclonal plasma antibody response. (G) SHM of expressed
964 mAbs by timepoint of isolation. (H) Binding of expressed mAbs to ancestral S, S1 subunit
965 and RBD. NB = non-binding. (I, J) mAb binding to ancestral S-protein (I) and avidity index
966 (J), plotted by timepoint of isolation, with previously characterized mAbs (Ctrl: CR3022,
967 B38, hACE2-Fc, C144, S309, S2M11, S2X333, COVA2-37) for comparison. (K) Heatmap
968 depicting binding and avidity information with predicted subunit binding for isolated and
969 control mAbs. Statistical analysis performed using non-parametric Mann-Whitney (Fig. E) or
970 Wilcoxon matched-pairs signed rank test (Fig. F, G, I, J). *$p < 0.05$. **$p < 0.01$. Data are
971 represented as mean ± SEM.

972

Figure 4: Tracking mRNA vaccines *in vivo* in non-human primates (A, B) *In vitro* uptake and translation of 0, 0.5 and 5 ug/mL mCitrine mRNA/LNPs in enriched primary human monocytes at 6, 24, 48 and 72 hours. Representative flow cytometry plots (A) and summarized data (B). (C) Non-human primates were immunized at 0 hours with saline, 10 ug or 100 ug mRNA/LNP. They were sacrificed 24 hours later and draining as well as non-draining tissues were collected and analyzed. (D) Representative flow cytometry plots of CD45+ immune cell infiltration in different tissues. (E) Enumeration of infiltrating cell subsets in different tissues. (F) Monocyte infiltration into the site of injection and draining lymph nodes. (G) Flow cytometry plots of LNP DiD and mCitrine signal in draining lymph nodes by innate cell subsets from saline- and vaccine-injected sites. (H) Proportion of vaccine-positive cells in different tissues by innate cell subset. (I) Vaccine-positive monocytes in primary, secondary and tertiary dLNs 24 hours after immunization. (J) Correlation between the number of infiltrating monocytes in the muscle and the number of vaccine-positive monocytes in primary and secondary draining lymph nodes. (K) Vaccine signal in different monocyte subsets and tissues at 24 hours. Statistical analyses were performed using a non-parametric Kruskal-Wallis test or Spearman correlation. *$p < 0.05$. **$p < 0.01$. ns = not significant. Data are represented as mean ± SEM.

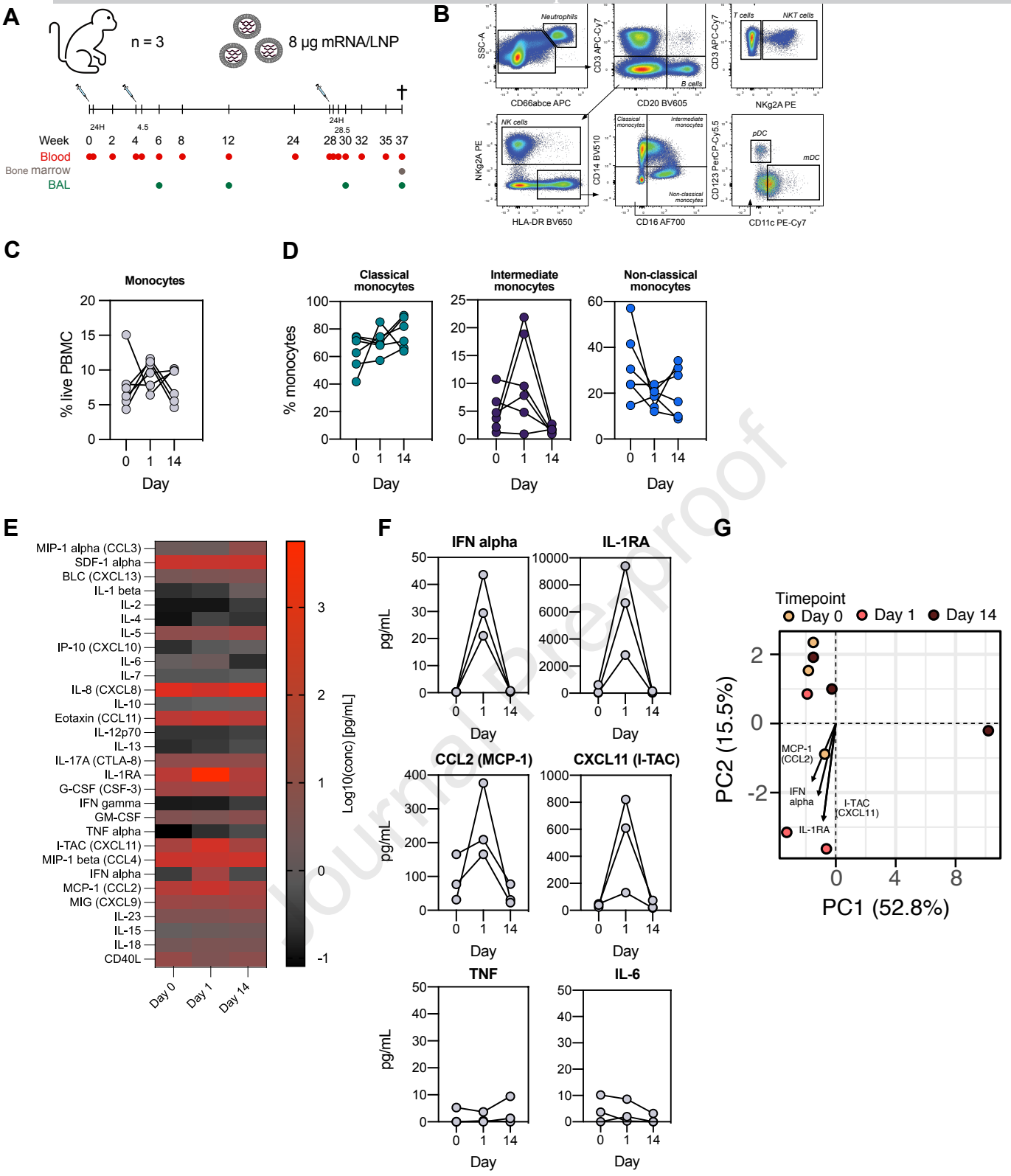

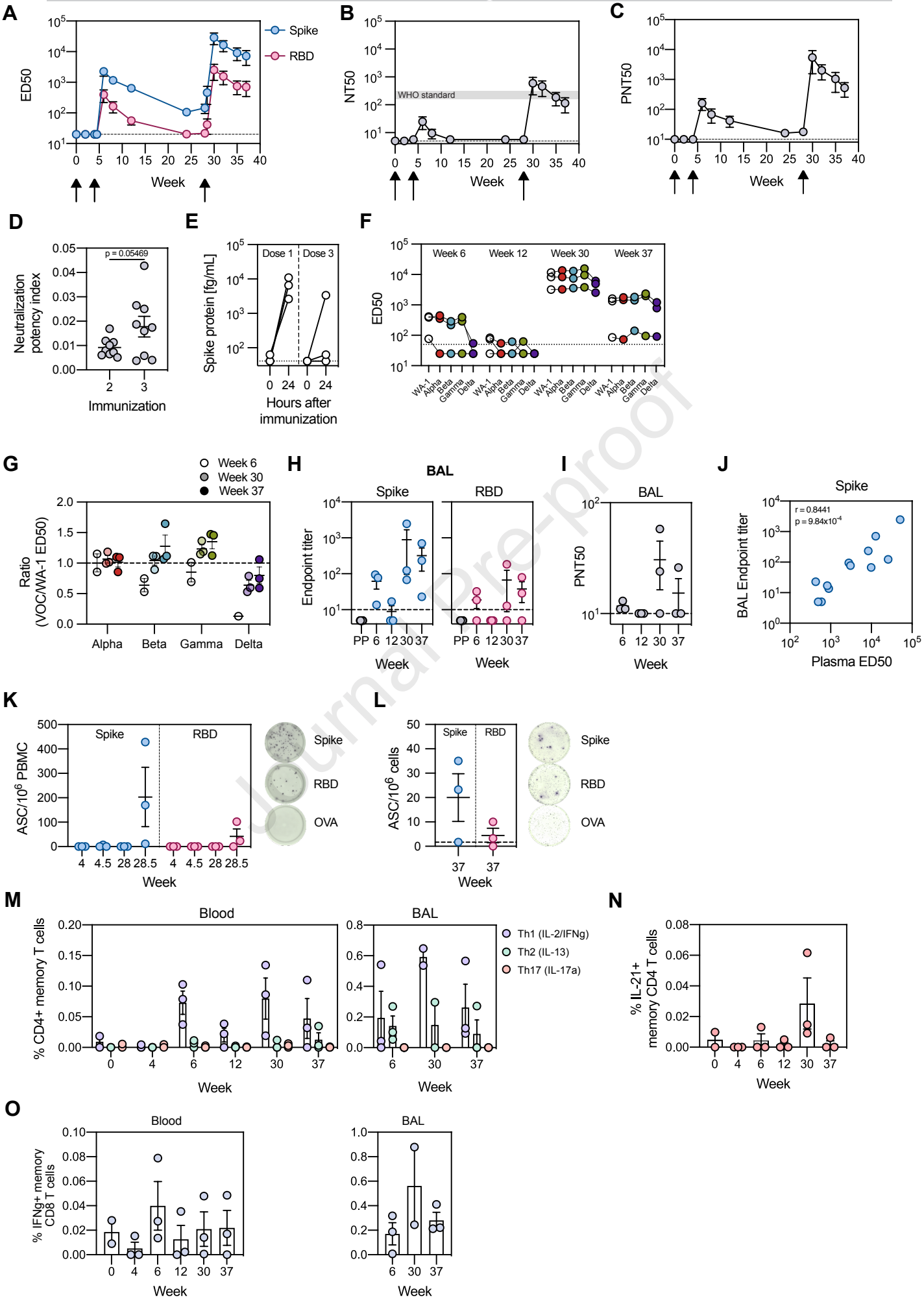

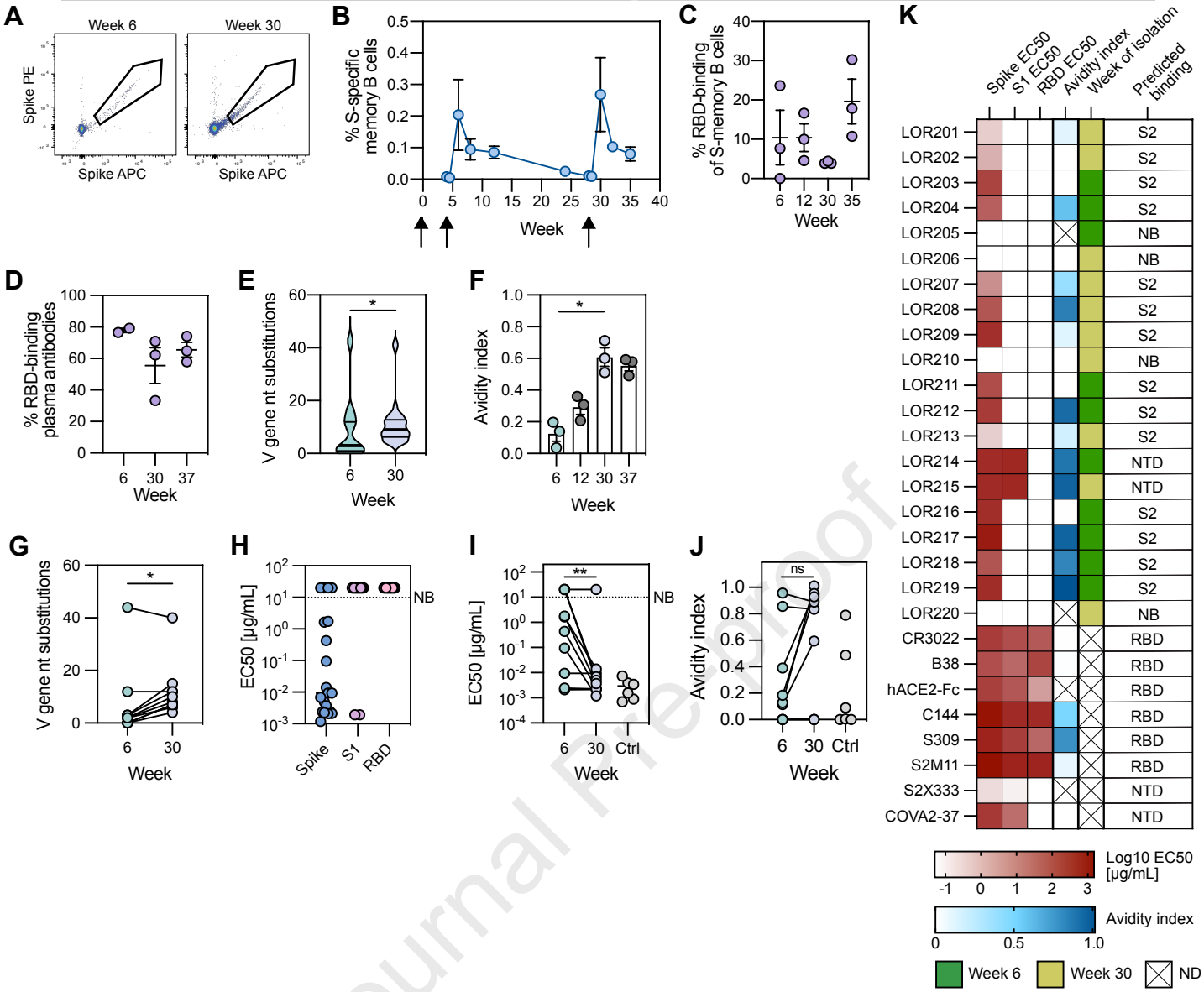

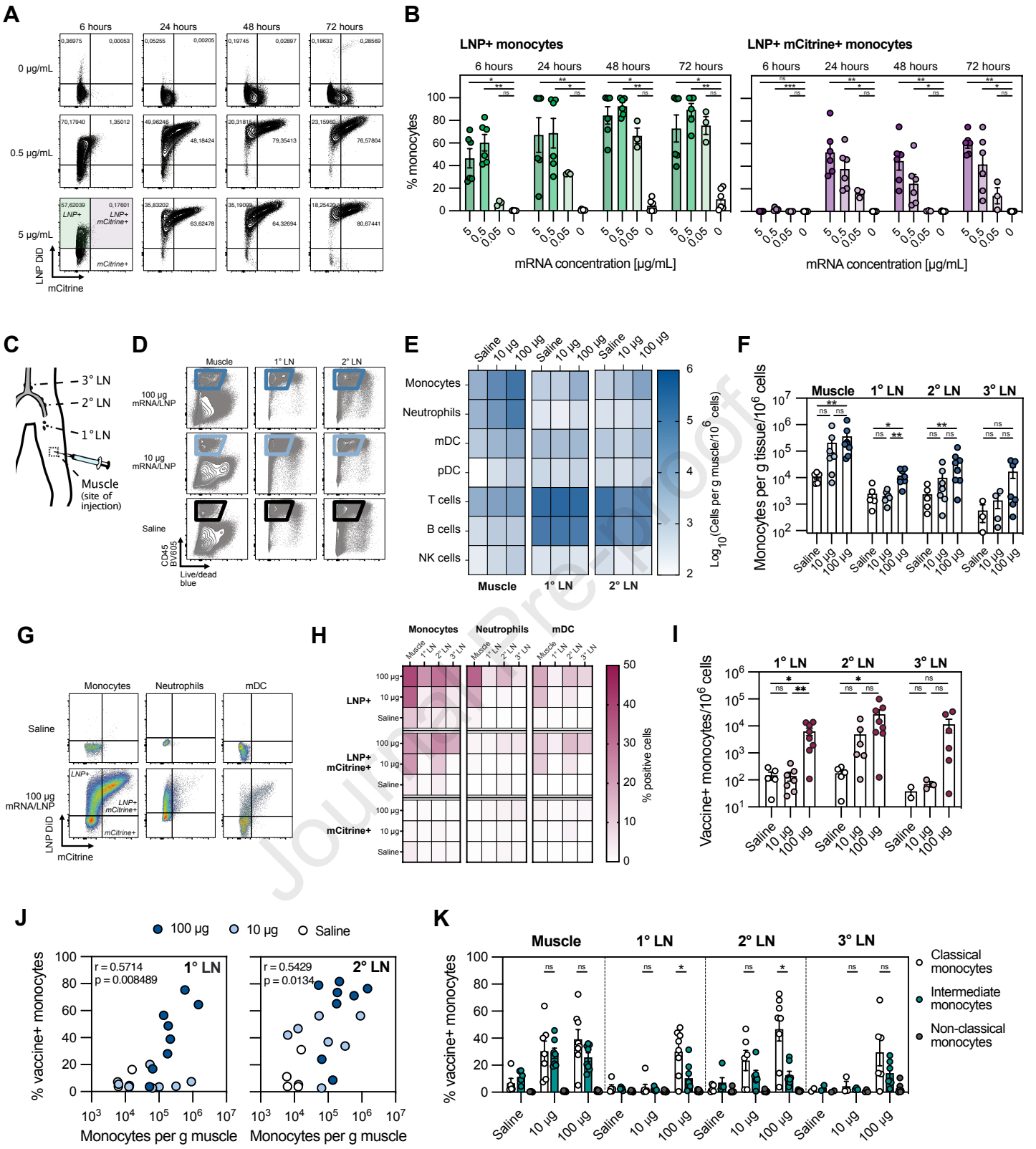
A
6 hours
24 hours
48 hours
72 hours
0 µg/mL
0.5 µg/mL
5 µg/mL
LNP DiD
mCitrine
B
LNP+ monocytes
LNP+ mCitrine+ monocytes
% monocytes
mRNA concentration [µg/mL]
C
3° LN
2° LN
1° LN
Muscle (site of injection)
D
Muscle
1° LN
2° LN
100 µg mRNA/LNP
10 µg mRNA/LNP
Saline
CD45 BV605
Live/dead blue
E
Monocytes
Neutrophils
mDC
pDC
T cells
B cells
NK cells
Log10(Cells per g muscle/10^6 cells)
F
Monocytes per g tissue/10^6 cells
G
Monocytes
Neutrophils
mDC
LNP+
LNP+ mCitrine+
mCitrine+
H
% positive cells
I
Vaccine+ monocytes/10^6 cells
J
100 µg
10 µg
Saline
% vaccine+ monocytes
r = 0.5714
p = 0.008489
r = 0.5429
p = 0.0134
Monocytes per g muscle
K
Classical monocytes
Intermediate monocytes
Non-classical monocytes

eTOC Synopsis

Lenart *et al* show significant improvement in magnitude and quality of vaccine-specific responses with the third low dose mRNA immunization. In biodistribution studies, low dose vaccines drained to fewer lymph node clusters compared to high dose, likely targeting fewer naïve lymphocytes and thus requiring multiple doses for induction of high-quality responses.